Nuclear Instruments and Methods in Physics Research B 494-495 (2021) 10–15

Contents lists available at ScienceDirect

Nuclear Inst. and Methods in Physics Research, B

journal homepage: www.elsevier.com/locate/nimb

Photocurrent improvement from magnetron DC sputtered and thermally treated ruthenium-based catalyst decoration onto $BiVO_4$ photoanodes

L.I. Gutierres [a,*], P. Migowski [b], I. Alencar [a,c], R.S. Thomaz [a], Adriano F. Feil [a]

[a] School of Technology, Pontifical University of Rio Grande do Sul, Brazil
[b] Institute of Chemistry, Federal University of Rio Grande do Sul, Brazil
[c] Department of Physics, Federal University of Santa Catarina, Brazil

ARTICLE INFO

Keywords:
Photoanode
Monoclinic bismuth vanadate
Water Splitting
Surface decoration
Ruthenium

ABSTRACT

Monoclinic $BiVO_4$ (BVO) properties favor its use as the main absorber in photoanodes applied for photoelectrochemical water splitting. However, hindrances as the high rate of recombination of the electrons and holes photogenerated and as the poor charge carrier transport limit its direct, practical use. Doping, building a heterojunction with other semiconductors and decorating the surface with catalysts like cobalt phosphate and ruthenium oxide are among the many existing approaches to improve BVO performance. The deposition of catalyst or cocatalyst normally involve the use of potentially hazardous techniques as chemical vapor deposition (CVD). In this work, we present a simple route for enhancing photoelectrochemical results in BVO samples. The decoration with metallic ruthenium is performed via magnetron sputtering DC, a reliable, inexpensive and safe-to-use physical deposition technique, followed by a thermal treatment in air within a muffle furnace for 6 h at 400 °C. A gain of about 45% in the photocurrent at 1.23 V vs reversible hydrogen electrode (RHE) and in the overall spectrum area in comparison with pristine BVO samples was registered by cyclic voltammetry measurements in a 0.5 M phosphate buffer solution under full spectrum illumination from a 100 W Xenon lamp. The morphological and chemical modifications that resulted in such photocurrent rise were characterized using Scanning Electron Microscopy (SEM), Rutherford Backscattering Spectrometry (RBS) and X-ray Photogenerated Spectroscopy (XPS).

1. Introduction

The electrical energy consumption is the cause to ca. 60% of the enhancement of the greenhouse effect, which confines heat in the atmosphere and contributes greatly to extreme climate changes that affect Earth [1]. One of the main alternatives to coal as a source to generating energy without harming the environment is the use the solar radiation in either physical or chemical processes, such as, respectively, photovoltaic (PV) and photoelectrochemical (PEC). The later, allow the solar PEC production of hydrogen and oxygen pure gases by splitting the water molecule into H_2 and O_2 and is one of the promising technologies with potential to providing clean, cost-effective, and domestically produced energy carrier, using the 120,000 TW of radiation that continually strikes the Earth's surface [2,3]. In order to initiate the solar water splitting (WS) reaction, a suitable semiconducting material has to be chosen to absorb the minimum energy necessary for this reaction to happen, the Gibbs free energy (237 $kJ.mol^{-1}$ or 1.23 V). The PEC device, once immersed in aqueous electrolyte, must also possess a series of desirable specific properties. The ideal absorbing material for a WS PEC device should encompass: suitable bandgap (E_g); valence (VB) and conduction (CB) band energies which enable the oxidation and the reduction of water; low charge recombination rate; being highly active for hydrogen evolution reaction (HER) and for oxygen evolution reaction (OER); and, among other properties, to easily and efficiently transfer charges from the semiconductor surface to the water molecule.

The ternary metal oxide $BiVO_4$ (BVO), is a material with promising prospects for PEC WS. BVO in the monoclinic phase is typically obtained as n-type semiconductor, with a $E_g \approx 2.4$ eV ($\lambda < 516$ nm), composed of relatively inexpensive elements, that has been widely used for several years as absorber of photoelectrodes in photoanodes for OER. Despite the several advantages, hindrances as the high rate of recombination of photogenerated electrons and holes and the poor charge carrier transport limits its unassisted use as sunlight absorber for PEC WS [4]. In order to overcome these undesired intrinsic characteristics, one may

* Corresponding author.
E-mail address: leandroize@gmail.com (L.I. Gutierres).

https://doi.org/10.1016/j.nimb.2021.03.002
Received 5 January 2020; Received in revised form 26 February 2021; Accepted 1 March 2021
Available online 11 March 2021

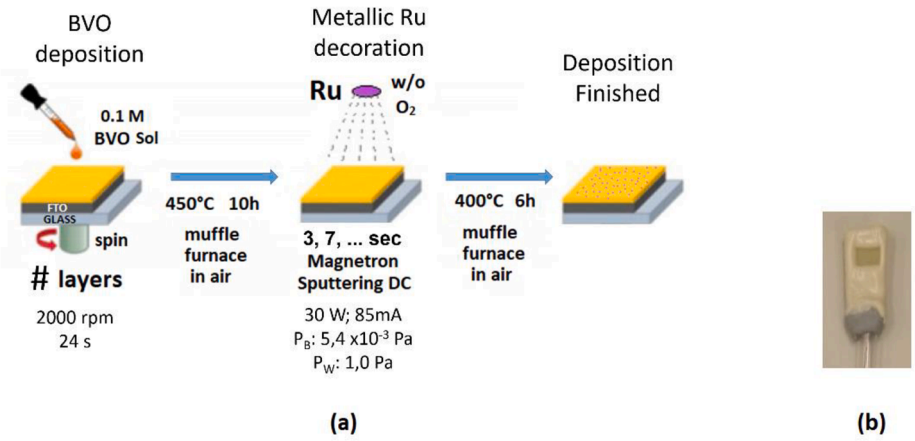

Fig. 1. (a) Deposition steps and parameters from the BVO layers until the decorated photoanode and (b) assembled photoelectrode.

modify the photoelectrode. Common approaches for increasing the PEC behavior of materials such as BVO are controlling size and shape of the semiconducting material, doping, forming heterojunctions with other metal oxides or decorating the surface with a catalyst [5,6]. As the OER has a high kinetic energy barrier due to the four-electron water oxidation reaction, it is normally the rate-limiting step of the PEC system. Therefore, catalyzing the OER is crucial and beneficial to the efficiency of the PEC WS process [7].

In order to achieve more efficient reactions within the solar water splitting process one may alter the surface of the photoanodes with the addition of OER electrocatalysts, such as cobalt phosphate, usually in the literature referred to as CoPi, Ferric Oxyhydride (FeOOH), Nickel oxide (NiO_x) and Ruthenium dioxide (RuO_2). The application of these materials yields more efficient photoelectrodes by improving the separation of the photogenerated electrons and holes and decreasing the kinetic barrier of the water oxidation, providing unique active sites with specific selectivity [4,8–10].

The techniques applied for depositing materials on the surface of photoelectrodes, such as atomic layer deposition (ALD), chemical vapor deposition (CVD), metal–organic deposition (MOD), and reactive sputtering, are usually complex, expensive or generate harmful side-products. Thus, it is of great importance to seek for alternative, ideally cheap, safe, easy to use and trustworthy methodologies for depositing PEC WS cocatalysers onto the surface of photoelectrodes. In this study, we have decorated the surface of BVO photoanodes with a ruthenium-based co-catalysts, deposited via DC magnetron sputtering, followed by thermal treatment in air at mild temperature. The PEC performance of the decorated BVO photoelectrodes was probed via cyclic voltammetry measurements and characterized with Scanning Electron Microscopy (SEM), Rutherford Backscattering Spectrometry (RBS) and X-ray Photogenerated Spectroscopy (XPS).

2. Materials and methods

2.1. Preparation of $BiVO_4$ photoanodes

For the deposition of the $BiVO_4$ (BVO), commercial FTO (fluorine-doped SnO_2) coated ($7°\Omega^{-2}$ sheet resistance) glass substrate, cut in approximately 1 in. square pieces, was cleaned in the following sequence: manually rubbing with a soft sponge soaked with Triton X100 5%; a couple of successive 10 min sonication baths in ethanol (99%) and acetone, followed by 10 more minutes of sonication in a 1 M KOH solution; and a final 20 min cleaning sonication in MiliQ water. After every cleaning step, the substrate was rinsed with MiliQ water and then dried with a thermal blower set to 90 °C. For the depositions of the BVO onto the clean transparent conductive FTO substrate, a solution made from 0.3631 g of bismuth(III) nitrate pentahydrate, $Bi(NO_3)_3$, dissolved in 3.75 ml of glacial acetic acid was add to a solution of vanadyl acetylacetonate, $VO(acac)_2$, 0.1989 g, dissolved in 25 ml of acetylacetone (≥99%), to obtain the dark green colored precursor solution. The

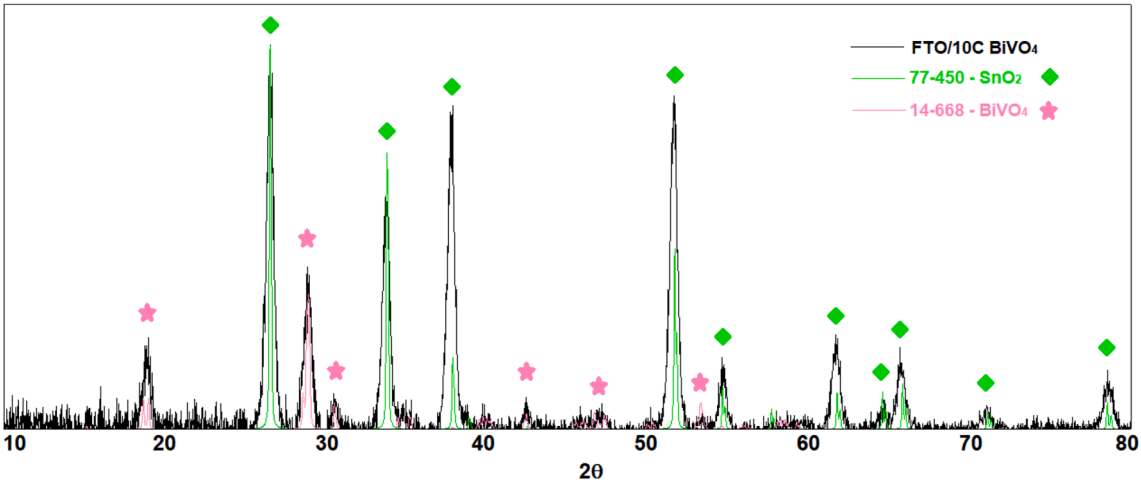

Fig. 2. X-Ray Diffraction (XRD) pattern of a 10 layer BVO photoanode (black line), deposited onto FTO, and the fitting curves and peaks of the SnO_2 (green diamond) and the $BiVO_4$ (pink star) crystallographic phases. (For interpretation of the references to colour in this figure legend, the reader is referred to the web version of this article.)

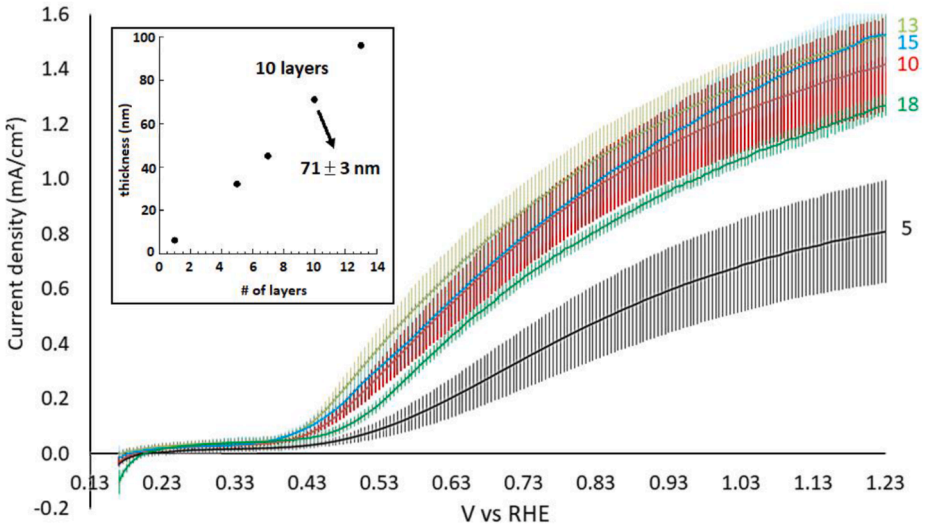

Fig. 3. Voltammetry curves under full spectrum irradiation of 1 sun in a 0.1 M K_2PO_4 with 0.2 M Na_2SO_3 electrolyte of the BVO samples with varying number (#) of layers: 5 (black line), 10 (red line), 13 (light green), 15 (light blue) and 18 (dark green). The insert depicts the thicknesses of BVO samples of 1, 5, 7, 10 and 13 layers, obtained via RBS. (For interpretation of the references to colour in this figure legend, the reader is referred to the web version of this article.)

substrate was mask along one of its borders with a 0.2 in. wide Kapton tape, so after the deposition of the BVO a direct electric contact to bare FTO was possible. The BVO deposition was performed in a layer-by-layer approach (from 5 up to 13 layers), by spin-coating ca. 200 μl of the precursor solution at 2000 rpm for 24 s (air purge), in a spinner model Spin150, from APT GmbH. As soon as the spinning deposition process of each layer was complete, the reminiscent solvent was evaporated by placing the samples for 10 min on a hot plate set to 350 °C. By the end of the deposition of the intended number of BVO layers, the whole batch was submitted to a thermal treatment in air, within a muffle furnace at 450 °C for 10 h.

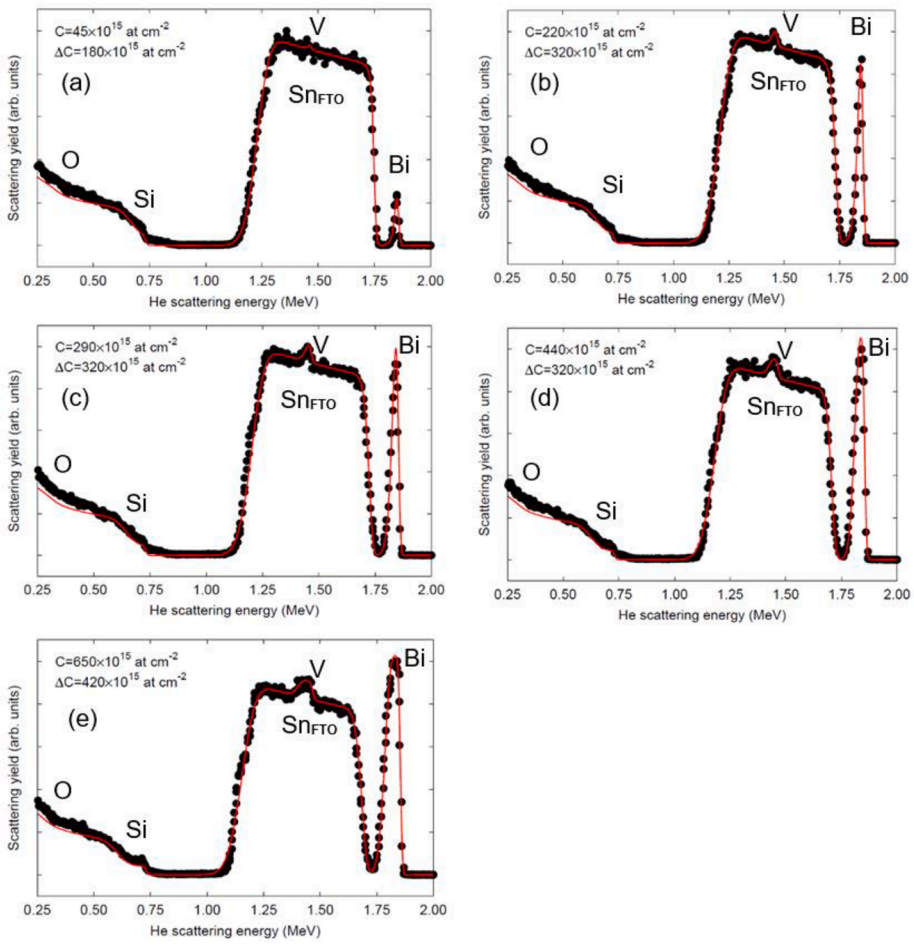

Fig. 4. Experimental RBS curves of the BVO samples deposited onto FTO in (a) 1 layer, (b) 5 layers, (c) 7 layers, (d) 10 layers, and (e) 13 layers, with the fitting curves from SIMNRA simulations (red lines). The thickness (C) and the roughness applied (ΔC) for each sample are included as the number of scattering centers per area. The regions corresponding to oxygen (O), Silicon (Si) from the glass under the FTO, tin from the FTO (Sn_{FTO}), and also vanadium (V), and bismuth (Bi) deposited are highlighted. (For interpretation of the references to colour in this figure legend, the reader is referred to the web version of this article.)

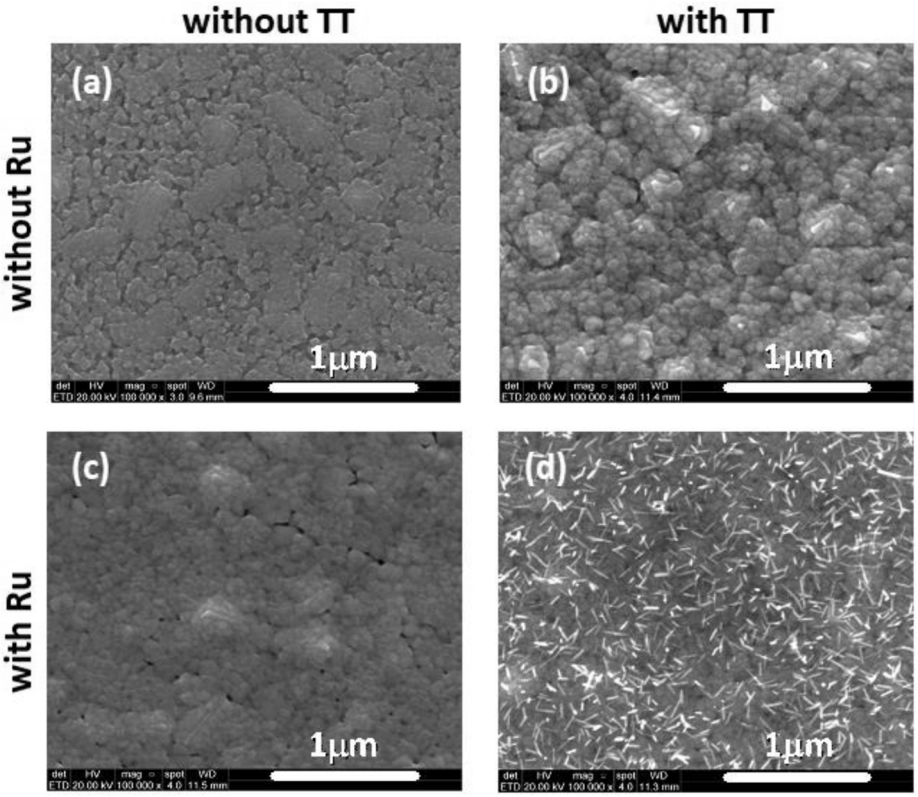

Fig. 5. Scanning Electron Microscopy (SEM) images depicting the surface morphology of BVO photoanodes (a) without Ru deposition and thermal treatment – TT; (b) without Ru and with TT; (c) with Ru and without TT; and (d) with Ru and with TT.

2.2. Preparation of Ru-decorated photoanodes

The deposition of the ruthenium (Ru) was performed using the magnetron DC sputtering technique in a chamber with inert atmosphere, filled with argon (purity 6.0, or >= 99.9999%), respectively at a base and working pressures of 5.4×10^{-3} Pa and 1.0 Pa. Ru was sputtered onto the samples from a Ru target (99.95% purity – AJA International) with 2 in. of diameter, and 6 mm thick, supplied with 85 mA, 320 V and 30 W, for 3, 7 and 14 s. Before placing the samples within the vacuum chamber, a mask was created in the borders using a 0.2 in. wide Kapton tape, for the later manufacturing of the photoanode's electric contact. After the Ru deposition, some of the samples were thermally treated in a muffle furnace for 6 h at 400 °C. Fig. 1a depicts the steps and parameters of each step from the BVO deposition until achieving the Ru decorated photoanode. After finishing all the steps described, samples which were not chosen for physical characterization were assembled, Fig. 1b, following international standards to allow testing the PEC performance when illuminated in a solar simulator under controlled conditions [2].

2.3. Characterization techniques and parameters

The PEC performance of the samples was registered using linear and cyclic voltammetry, with a Gamry potensiostat (model Interface 1000), at 100 mV/s scan rate, with a 5 mV step size, up to a 200 mA maximum current, using a 100 $mW.cm^{-2}$ Xenon lamp at full spectrum (1 sun at normal incidence; distance calibrated with a standardized Si solar cell). The PEC behavior of each type of photoelectrode was measured for three different samples and linear sweep curves shown below depict the variance of the set experiments. For the non-decorated BVO samples, the electrolyte was a mixture of 0.1 M K_2HPO_4 and 0.2 M Na_2SO_3. Meanwhile, for the Ru-decorated samples, voltammetry measurements were performed in a 0.5 M Phosphate Buffer Solution (PBS) at pH 6.7. Reference and counter electrodes were, respectively, Ag/AgCl and a platinum coiled-wire. In order to confirm the BVO monoclinic phase of the samples, X-Ray Diffraction (XRD) was performed using a Bruker D8 advanced diffractometer in Bragg-Brentano configuration operating at 40 kV and 30 mA, from 10° up to 90°, with 0,02° of increment, 2° per minute scan speed, with a copper K-alpha filament. Rutherford Backscattering Spectrometry (RBS) was applied for determining the thickness of the multilayered BVO films and to investigate both the FTO/BVO/Ru, and a simpler Si/Ru systems. For the RBS measurements, a 2 MeV He^+ beam delivered from a 3 MV Tandetron (High Voltage Engineering) impinged at normal incidence to the surface of the samples. The scattered ions were collected at an angle of 165°with a surface-barrier, silicon charged-particle detector (17 keV resolution). Channel-to-energy conversion was performed using the high-energy edge signal from ions backscattered at a gold standard specimen. Data were analyzed using the SIMNRA software [11] varying the layer parameters *Thickness* and *FWHM* of thickness distribution, both in atoms per square centimeter. No roughness was attributed to the glass or silicon substrates. FTO roughness was obtained from data measured on samples with no deposition, while BVO and Ru roughness were included in order to improve the fitting. From the crystallographic data, Bragg reflections agree for both deposited films and bulk materials, indicating the density of the films are not strongly different from the bulk materials. This allows the thickness conversion from atoms per square centimeter to nanometers, as in the data shown in the inset of Fig. 3. Scanning Electron Microscopy (SEM) was used to characterize the morphology of the samples' surface, with the beam set to 10 kV up to 20 kV. For the spectroscopic analysis of the samples using X-Ray Photoelectron Spectroscopy (XPS) an Omicron surface analyzer, equipped with a static electron energy analyzer Sphera with a Mg (225 W) source was used. The Voltammetry, XRD and SEM characterizations were performed at the Pontifical Catholic University of Rio Grande do Sul, Brazil, while the RBS and XPS measurements were done in the Federal University of Rio Grande do Sul, Brazil.Fig. 4.

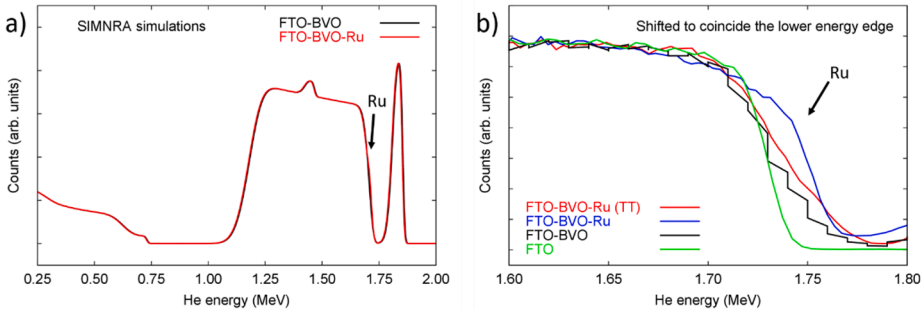

Fig. 6. Subtle distinction of Ru content apparent in RBS data (a) SIMNRA simulations for the $BiVO_4$ (BVO) film deposited onto an FTO-doped glass substrate (black line) and for the same system decorated with Ru (red line), and (b) experimental results for the energy region of Ru surface signal for FTO (green line), FTO/BVO (black line), FTO/BVO/Ru (blue line) and FTO/BVO/Ru with TT (red line) systems. Low energy edge of the Sn signal was shifted to coincide in all spectra for the sake of comparison. (For interpretation of the references to colour in this figure legend, the reader is referred to the web version of this article.)

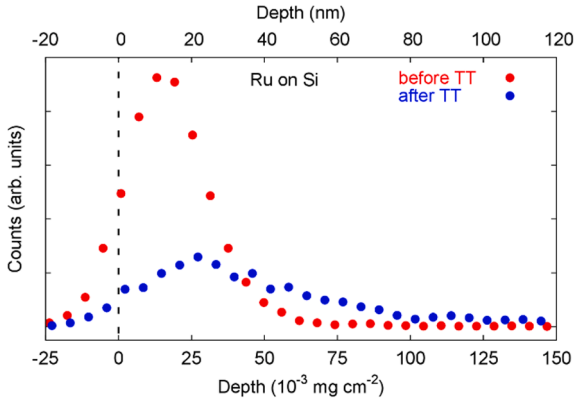

Fig. 7. Depth profile of Ru sputtered (3 s) onto Si substrate, before (red dots) and after (blue dots) thermal treatment (TT) at 400 °C for 6 h, depicting both the significant loss and the slight diffusion of the Ru content after TT. (For interpretation of the references to colour in this figure legend, the reader is referred to the web version of this article.)

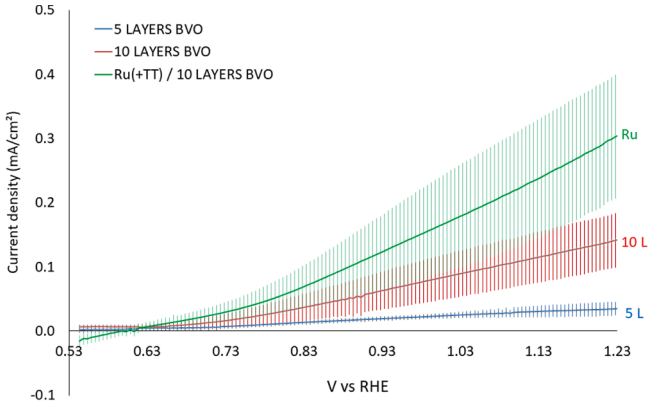

Fig. 8. Voltammetry curves under full spectrum irradiation of 1 sun in a phosphate buffer electrolyte (pH 6.7) of the Ru decorated (with thermal treatment – TT) BVO photoanode (green) in comparison to the BVO photoanodes with 5 (blue) and 10 (red) layers. (For interpretation of the references to colour in this figure legend, the reader is referred to the web version of this article.)

3. Results

For studying the PEC results and the feasibility of decorating the BVO photoanodes with Ru-based catalyst, first, from 5 up to 18 layers of BVO deposited onto FTO coated transparent substrate were submit to series of voltammetry measurements in a solution of 0.1 M K_2HPO_4 and 0.2 M Na_2SO_3. Before optimizing the number of BVO layers, XRD results, Fig. 2, confirmed the presence of the monoclinic (m-BVO) phase, and of the SnO_2 from the substrate [12]. Cyclic voltammetry measurements of BVO photoelectrodes under illumination, Fig. 3, point similar curves for the samples with 10–15 layers, considering the variance observed at 1.23 V vs RHE. Samples with 5 and 18 layers yield the lowest photoactivities, due to the low absorption length, 5 layers, and to the high thickness, 18 layers, that hinders the charge carriers to reach the circuit. From these findings, we have chosen to decorate BVO photoanodes with 10 layers. As the elemental composition of the samples was known, RBS spectra were used for measuring the aerial concentration of scattering centers in each sample (i.e. the product between sample density and thickness). Thicknesses were calculated assuming bulk density for the layers. The thicknesses of the BVO films as a function of the number of layers deposited is depicted in the inset of Fig. 3.

The fitting of the RBS curves from the BVO samples of 1, 5, 7, 10 and 13 layers are shown in Error: Reference source not found. The peaks of Bi and V increase in intensity and in width when more layers are deposited. The morphology of the BVO photoanodes with and without the Ru decoration (3 s), and with and without thermal treatment (TT), is shown in Fig. 5. The presence of rod-like structures is attributed to be composed of Ru, as these structures were only observed in samples in which Ru was sputtered and thermally treated. Clearly, a 3-second-long sputtering was not sufficient to create even a nanometric layer of Ru. Simulations of RBS spectra of the FTO-BVO system with and without Ru (Fig. 6a) demonstrate how subtle is the distinction between the preexisting Sn edge and the Ru signal in this case. By analyzing the energy range corresponding to the Ru content in the RBS spectra of FTO, FTO/BVO, FTO/BVO/Ru and FTO/BVO/Ru with TT shifted to match the lower energy edge of the Sn signal, as in Fig. 6b, one may identify the presence of Ru in both scenarios, with and without TT. Additionally, a reduction of the Ru signal after the TT in the target system is observed. In a simpler Si/Ru system, the depth profile with and without TT (Fig. 7) depicts both the loss and the diffusion of Ru content after the TT. RBS analysis of Ru deposition for 7 and 14 s onto BVO photoanodes were attempted, but the voltammetry curves indicate that no semiconductor-electrolyte junction was built, once dark and illuminated voltammetry measurements were similar. Also, all photoanodes with Ru but without TT did not present photoactivity under illumination. The photoanodes with 3 s of Ru and thermal treatment increased the current density by 45% at 1.23 V vs RHE (reversible hydrogen electrode – a standard reference electrode for electrochemical processes), in a 0.5 M phosphate buffer solution (PBS) with pH 6.7, in comparison to BVO samples with 10 layers (Fig. 8).

XPS spectra analysis of a Si/Ru sample without TT was performed following to the model developed by Morgan and coworkers [13], as shown in Fig. 9, and indicate, from the O1s region (FWHM of 2.035 to all peaks), which has a shoulder at the lower binding energy range which fits two single O bonds, the presence of RuO_2 (Fig. 9b) [13–16]. Ribera and coworkers [17] have reported on the dual layer (surface and subsurface) oxidation of metallic ruthenium films thermally oxidized at temperatures ranging from 150 °C up to 500 °C for different times. The longer the thermal treatment, the more Ru metal should be oxidized and denser RuO_2 is formed, with a slight increase on the content of low

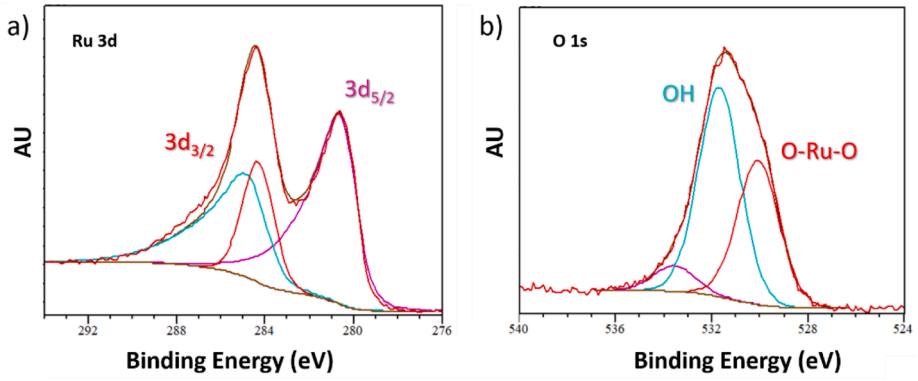

Fig. 9. X-ray Photoelectron Spectroscopy (XPS) spectra in arbitrary units (AU) from the regions corresponding to the binding energies of the (a) Ru ($3d_{3/2}$ and $3d_{5/2}$) and (b) O (O1s) before thermal treatment.

density RuO_2 quickly reaching a plateau. Nevertheless, due to the short range in depth of the XPS technique, the data of the Si/Ru system after the 400 °C for 6 h thermal treatment indicates a strong reduction in the presence of Ru on the surface of the sample.

4. Conclusions

A low cost and reproducible method has been proposed and developed as alternative to the commonly applied techniques for catalyzing through decorating the surface of photoanodes, here with a ruthenium-based decoration of $BiVO_4$ films. The route encompassing the ultrafast deposition via magnetron sputtering DC in inert atmosphere, followed by thermal treatment at mild temperature in a muffle furnace, uses non-expensive apparatus and yield a great improvement of 45% in the current density at the potential for water splitting. XPS analysis point to the presence of RuO_2 after the 3 s deposition in argon atmosphere. RBS data was not as sensitive as the XPS for the same sample but was able to track the behavior of the Ru content after the 400 °C for 6 h thermal treatment in air. Although the XPS findings could not confirm the presence of Ru, or RuO_2, after TT, as the technique has very short depth resolution due to the X-Ray energy applied, one cannot state Ru has all simply vaporized with TT. The RBS spectra indicate that, despite a great fraction of Ru has vanished after TT, another traceable part may have diffused within the surface of the BVO, contributing to the creation of active sites for the photoelectrochemical reactions, being then the source of the improvement achieved in the current density measurements in PBS.

Declaration of Competing Interest

The authors declare that they have no known competing financial interests or personal relationships that could have appeared to influence the work reported in this paper.

Acknowledgments

The authors acknowledge the financial support given by the Brazilian Government division CAPES (Coordenação de Aperfeiçoamento de Pessoal de Nível Superior), FAPERGS, CNPq, Finep and the support given by the French Vacuum Society (SFV) during the IBA conference. PM would like to thank Universidade Federal do Rio Grande do Sul for support with PROPESQ/UFRGS – PROGRAMA INSTITUCIONAL DE AUXÍLIO À PESQUISA DE DOCENTES RECÉM-CONTRATADOS and CNPq for the "BOLSA ATRAÇÃO DE JOVENS TALENTOS - BJT 2014 Processo N° 401063/2014-3". Prof. Dr. Claudio Radtke, from the Federal University of Rio Grande do Sul, Brazil, is acknowledge for the XPS measurements and fruitful discussions.

References

[1] Y.P. Hua, M. Oliphant, E.J. Hu, Development of renewable energy in Australia and China: A comparison of policies and status, Renewable Energy 85 (2016) 1044–1051.
[2] Z. Chen, H. Dinh, E. Miller, Photoelectrochemical Water Splitting: Standards, Experimental Methods, and Protocols, Springer, New York, 2013.
[3] C. United States. Department of Energy. Basic Energy Sciences Advisory and L. Oak Ridge National, Basic Research Needs to Assure a Secure Energy Future: A Report. Oak Ridge National Laboratory, 2003.
[4] S. Hernández, G. Gerardi, K. Bejtka, A. Fina, N. Russo, Evaluation of the charge transfer kinetics of spin-coated BiVO4 thin films for sun-driven water photoelectrolysis, Appl. Catal. B: Environ. 190 (2016) 66–74.
[5] S. Cho, J.W. Jang, K.H. Lee, J.S. Lee, Research Update: Strategies for efficient photoelectrochemical water splitting using metal oxide photoanodes, Apl. Mater. 2 (2014) 1.
[6] S.S.M. Bhat, S.A. Lee, J.M. Suh, S.P. Hong, H.W. Jang, "Triple Planar Heterojunction of SnO2/WO3/BiVO4 with Enhanced Photoelectrochemical Performance under Front Illumination," (in English), Appl. Sci.-Basel 8 (2018) 10.
[7] X. Yao, et al., "Scale-Up of BiVO4 Photoanode for Water Splitting in a Photoelectrochemical Cell: Issues and Challenges," (in English), Energy Technol. 6 (1) (2018) 100–109.
[8] G. Ge, et al., Ultrathin FeOOH nanosheets as an efficient cocatalyst for photocatalytic water oxidation, J. Mater. Chem. A 7 (15) (2019) 9222–9229.
[9] J.H. Kim, et al., Palladium oxide as a novel oxygen evolution catalyst on BiVO4 photoanode for photoelectrochemical water splitting, J. Catal. 317 (2014) 126–134.
[10] C. Zachaus, F.F. Abdi, L.M. Peter, R. van de Krol, Photocurrent of BiVO4 is limited by surface recombination, not surface catalysis, Chem. Sci. 8 (5) (2017) 3712–3719.
[11] M. Mayer, SIMNRA User's Guide, Report IPP 9/113, Max-Planck-Institut für Plasmaphysik, Garching, Germany, 1997.
[12] A. Chemseddine, K. Ullrich, T. Mete, F.F. Abdi, R. van de Krol, Solution-processed multilayered BiVO4 photoanodes: influence of intermediate heat treatments on the photoactivity, J. Mater. Chem. A 4 (5) (2016) 1723–1728.
[13] H.Y.H. Chan, C.C. Takoudis, M.J. Weaver, High-pressure oxidation of ruthenium as probed by surface-enhanced Raman and X-ray photoelectron spectroscopies, J. Catal. 172 (2) (1997) 336–345.
[14] D.J. Morgan, Resolving ruthenium: XPS studies of common ruthenium materials, Surf. Interface Anal. 47 (11) (2015) 1072–1079.
[15] Q.F. Wang, X. Liang, Y. Ma, D.H. Zhang, Fabrication of hollow nanorod electrodes based on RuO2/Fe2O3 for an asymmetric supercapacitor, Dalton Trans. 47 (23) (2018) 7747–7753.
[16] C. Mun, J. Ehrhardt, J. Lambert, C. Madic, "XPS investigations of ruthenium deposited onto representative inner surfaces of nuclear reactor containment buildings," (in English), Appl. Surf. Sci. 253 (18) (2007) 7613–7621.
[17] R.C. Ribera, R.W.E. van de Kruijs, S. Kokke, E. Zoethout, A.E. Yakshin, F. Bijkerk, Surface and sub-surface thermal oxidation of thin ruthenium films, Appl. Phys. Lett. 105 (2014) 13.